Ideal and defective vertex configurations in the planar octagonal quasilattice

M. Baake
Institut für Theoretische Physik, Universität Tübingen, Auf der Morgenstelle 14, D-7400 Tübingen, Germany
and Department of Physics, University of Tasmania, GPO Box 252C, Hobart Tas 7001, Australia

D. Joseph
Institut für Theoretische Physik, Universität Tübingen, Auf der Morgenstelle 14, D-7400 Tübingen, Germany
(Received 6 June 1990)

The well-known two-dimensional octagonal quasilattice is realized by means of dualization and Klotz construction. We discuss the geometric properties and the extended symmetry of the pattern. The concept of geometric defects is introduced, and an elastic energy measure ΔE is presented that allows a simple sequencing of the forbidden vertices. After a sketchy comparison with Lennard-Jones calculations, some thermodynamic consequences of ΔE are discussed. It turns out that the specific heat should show a significant increase in comparison with the crystallographic case.

I. INTRODUCTION

Quasiperiodic patterns as obtained by projection from higher-dimensional periodic structures have proved useful for the description of quasicrystalline materials,[1] providing the noncrystallographic counterpart of the cell models of ordinary crystallography. Additionally, they have also attracted considerable research activity from the geometric point of view.[2] This geometry, however, is not an esoteric part of the game but an extremely powerful method for the analysis of structure models. Not only effective algorithms for the explicit construction of quasilattices can be obtained that way[3] but also their local structures like possible vertices and their frequencies, their configurational neighborhood,[4,5] and, last but not least, a straightforward approach to the kinematic factor of the Fourier theory.[6,7]

An essential tool is provided in the form of the dualization method together with the Klotz construction,[8,9] where the perpendicular space plays an important role for the determination of geometric properties. However, this structure can only fully determine the case of ideal quasilattices, i.e., defect-free ones. Since real material shows significant defect contributions, the latter have to be included in the description. The standard approach uses the Landau theory of phase transitions[10,11] via the additional degrees of freedom of the free energy, called phasons, and treats the pattern either as an ideal one with phasonic defects or directly as a random tiling[12] with configurational entropy.

Although this procedure seems to be quite successful, we would like to present a complementary picture based on the geometry or, more precisely, on the dualization that is herited from the defect-free case and turns out to be much more powerful than expected. The advantage of this procedure is the reduction of the basic assumptions renouncing the (phenomenological) Landau theory.

In order to explain our approach, we have chosen the well-known planar octagonal quasilattice[13] because it combines an easy description with a good graphical presentability but does not suffer from the degenerate properties of 1-D patterns like the Fibonacci chain, e.g., the lack of nontrivial symmetries and real matching conditions. Obviously, several results that are well-known from the literature[13–16] are rederived in what follows, but this time merely for pedagogical reasons because we hope that the understanding of the dualization scheme is facilitated that way. An additional treatment of another octagonal phase that can be linked to the dodecagonal one is planned to be presented in the future.[17]

The paper is organized as follows. In Sec. II, we rederive the primitive octagonal quasilattice with use of the dualization scheme and Klotz construction. Special attention is paid to the symmetry and the local properties of the pattern. A very efficient tile-by-tile production algorithm is presented. The vertex configurations of the ideal pattern and their frequencies are derived, followed by a treatment of the ten forbidden vertices—called geometric defects of the first kind—within the dualization scheme in Sec. III. Based on the geometric analysis in perpendicular space, an elastic measure for the vertices is proposed that can be interpreted as a mean-field approach to the contribution of defects to the total energy. This energy measure is justified by a comparison with stability calculations for a simple two-atom decoration with truncated Lennard-Jones potentials.

In Sec. IV, the elastic energy measure serves as input to some simplistic thermodynamics in a canonical ensemble. The degrees of freedom that stem from the geometric defects of the first kind result in an additional contribution to the specific heat that, depending on the fundamental excitation energy, should be seen as a measurable effect.

In the Appendix, we briefly perform the same program for the Fibonacci chain with use of an exact mapping to a one-dimensional (1D) antiferromagnetic Ising model with a transversal magnetic field that is exactly solvable. That

way, one can get some insight in the approximations that are necessary for the treatment of the 2D example.

II. THE OCTAGONAL QUASILATTICE

Although the octagonal quasilattice and its construction from the grid method or the cut-and-project prescription is well-known in the literature[13–15] we will start with a description of this quasilattice that is based on the rigorous dualization scheme and Klotz construction.[8,9] Considering the 4D primitive hypercubic lattice $\mathbb{Z}^4$ the octagonal pattern is derived from, one finds two natural tilings of 4D space by congruent hypercubes

(a) the central Voronoi domain

$$V(\mathbf{0}) \equiv \{\mathbf{x} \in \mathbb{R}^4 \,|\, |\mathbf{x}_i| \leq \tfrac{1}{2}, i = 1, \ldots, 4\} \tag{2.1}$$

and

(b) the closed primitive unit cell

$$\{\mathbf{x} \in \mathbb{R}^4 \,|\, 0 \leq \mathbf{x}_i \leq 1, i = 1, \ldots, 4\} \ , \tag{2.2}$$

together with their images under the translation group $T_{\mathbb{Z}^4}$. Including the hierarchy of the boundaries, one obtains the Voronoi complex $\mathcal{V}$ and the dual complex $\mathcal{V}^*$, respectively. It is an important feature of this construction that to every boundary P of $\mathcal{V}$ of dimension $0 \leq m \leq 4$ there exists a uniquely determined boundary P^* of dimension $4-m$ with the properties (i) P and P^* are perpendicular to each other and (ii) P and P^* intersect each other at precisely one point.

For more details on the dualization method see Refs. 8 and 9. Here, the 2D boundaries of $\mathcal{V}$ and $\mathcal{V}^*$, which all have the shape of squares, are important because they are the preimages of the cells of the quasicrystal. Since $\mathcal{V}$ and $\mathcal{V}^*$ are congruent as cell complexes, it does not matter which complex we start from for the construction of the pattern—both versions will be congruent.

Before we can proceed, we have to choose a 2D physical space by the demand of eightfold symmetry. The holohedry of the lattice $\mathbb{Z}^4$ is the hyperoctahedral group $\Omega(4)$ (Refs. 18, 19) that does not admit a proper invariant subspace. However, the dihedral group D_8, generated by $(\mathbf{g}_8)^8 = \mathbf{s}^2 = \mathbf{e}$ with

$$R(\mathbf{g}_8) \equiv \begin{bmatrix} 0 & 0 & 0 & -1 \\ 1 & 0 & 0 & 0 \\ 0 & 1 & 0 & 0 \\ 0 & 0 & 1 & 0 \end{bmatrix}, \quad R(\mathbf{s}) \equiv \begin{bmatrix} 1 & 0 & 0 & 0 \\ 0 & 0 & 0 & -1 \\ 0 & 0 & -1 & 0 \\ 0 & -1 & 0 & 0 \end{bmatrix} , \tag{2.3}$$

does. The characters of D_8 (Ref. 20) are given in Table I. In fact, the representation R splits into two inequivalent 2D irreps,

$$UR(\mathbf{g})U^{-1} = R^{\mathrm{red}}(\mathbf{g}), \quad \mathbf{g} \in D_8 \ , \tag{2.4}$$

$$R^{\mathrm{red}}(\mathbf{g}_8) \equiv \begin{bmatrix} c & -s & 0 & 0 \\ s & c & 0 & 0 \\ 0 & 0 & c' & -s' \\ 0 & 0 & s' & c' \end{bmatrix} ,$$

$$R^{\mathrm{red}}(\mathbf{s}) \equiv \mathrm{diag}(1, -1, 1, -1) \ , \tag{2.5}$$

with

$$c \equiv \cos\left[\frac{2\pi}{8}\right], s \equiv \sin\left[\frac{2\pi}{8}\right] ,$$

$$c' \equiv \cos\left[\frac{6\pi}{8}\right], s' \equiv \sin\left[\frac{6\pi}{8}\right] ,$$

and

TABLE I. The irreducible characters of the dihedral group D_8.

Class / irreps	$\{\mathbf{e}\}$	$\{\mathbf{r}^k, \mathbf{r}^{-k}\}$ $k=1,2,3$	$\{\mathbf{r}^4\}$	$\{\mathbf{s}, \mathbf{sr}^2, \ldots, \mathbf{sr}^6\}$	$\{\mathbf{sr}, \mathbf{sr}^3, \ldots, \mathbf{sr}^7\}$
ψ_1	1	1	1	1	1
ψ_2	1	1	1	−1	−1
ψ_3	1	$(-1)^k$	1	1	−1
ψ_4	1	$(-1)^k$	1	−1	1
ρ_1	2	$2\cos\left[k\frac{2\pi}{8}\right]$	−2	0	0
ρ_2	2	$2\cos\left[2k\frac{2\pi}{8}\right]$	2	0	0
ρ_3	2	$2\cos\left[3k\frac{2\pi}{8}\right]$	−2	0	0

$$U \equiv \sqrt{\tfrac{1}{2}} \begin{bmatrix} 1 & \sqrt{\tfrac{1}{2}} & 0 & -\sqrt{\tfrac{1}{2}} \\ 0 & \sqrt{\tfrac{1}{2}} & 1 & \sqrt{\tfrac{1}{2}} \\ 1 & -\sqrt{\tfrac{1}{2}} & 0 & \sqrt{\tfrac{1}{2}} \\ 0 & \sqrt{\tfrac{1}{2}} & -1 & \sqrt{\tfrac{1}{2}} \end{bmatrix} . \tag{2.6}$$

The representation spaces are called $\mathbb{E}_\parallel$ and $\mathbb{E}_\perp$, respectively. The projection of the 4D basis vectors into these two subspaces is shown in Fig. 1. We identify $\mathbb{E}_\parallel$, where the eightfold element appears as rotation by 45°, with the physical space. It turns out that the D_8, which has 16 elements, is the maximal subgroup of $\Omega(4)$ compatible with the decomposition $\mathbb{R}^4=\mathbb{E}_\parallel+\mathbb{E}_\perp$ (a different statement in Ref. 14 is incorrect).

Now, that $\mathbb{E}_\parallel$ is fixed by group theoretic demands, we can define the pattern as follows. Fix a vector $\mathbf{c}_\perp \in \mathbb{E}_\perp$. Whenever a 2D boundary P of the Voronoi complex intersects with $\mathbb{E}_\parallel+\mathbf{c}_\perp$ [which is tantamount with $\mathbf{c}_\perp \in \pi_\perp(P)$], we have to project P^*, the dual 2D boundary, into $\mathbb{E}_\parallel$, i.e., the pattern $\mathcal{O}$ is

$$\mathcal{O}(\mathbf{c}_\perp)=\{\pi_\parallel(P^*) | P \text{ a 2D boundary of } \mathcal{V} \text{ and } \mathbf{c}_\perp \in \pi_\perp(P)\} . \tag{2.7}$$

If $\mathbf{c}_\perp$ is not contained in the projection image $\pi_\perp(P^1)$ of a 1D boundary P^1 of $\mathcal{V}$, $\mathcal{O}(\mathbf{c}_\perp)$ is a proper space filling of $\mathbb{E}_\parallel$, i.e., without gaps or overlaps.[8,9] They all belong to the same local isomorphism class of the so-called planar octagonal quasilattice as introduced by Beenker[13] via the grid method.

By means of the dualization scheme, we can immediately conclude the set of vertices of $\mathcal{O}(\mathbf{c}_\perp)$ to be

$$\{\pi_\parallel(\mathbf{q}) | \mathbf{q} \in \mathbb{Z}^4, \mathbf{c}_\perp \in \pi_\perp(V(\mathbf{q}))\} , \tag{2.8}$$

where $V(\mathbf{q})$ is the Voronoi domain of $\mathbb{Z}^4$ around the lattice point $\mathbf{q}$. Since $V(\mathbf{q})=V(\mathbf{0})+\mathbf{q}$ the vertex set takes the form

$$\{\pi_\parallel(\mathbf{q}) | \mathbf{q} \in \Gamma, [\mathbf{c}_\perp - \pi_\perp(\mathbf{q})] \in \pi_\perp(V(\mathbf{0}))\} . \tag{2.9}$$

The next step is the determination of the vertex configuration around a vertex point. Obviously, the tiles surrounding $\pi_\parallel(\mathbf{q})$ are those $\pi_\parallel(P^*)$, $P \in \mathcal{V}$ with $\dim(P)=2$, which obey $P-\mathbf{q} \in V(\mathbf{0})$ and $\mathbf{c}_\perp - \pi_\perp(\mathbf{q}) \in \pi_\perp(P)-\mathbf{q}$. Constructing a concrete pattern now means (1) find all $\mathbf{q} \in \mathbb{Z}^4$ such that $\mathbf{c}_\perp - \pi_\perp(\mathbf{q}) \in \pi_\perp(V(\mathbf{0}))$, i.e., the vertex points. (2) For each vertex point, take every 2D boundary P of $V(\mathbf{0})$ with $\mathbf{c}_\perp - \pi_\perp(\mathbf{q}) \in \pi_\perp(P)$; then $\pi_\parallel(\mathbf{q})+\pi_\parallel(P^*)$ belongs to the pattern. We see that for the whole analysis of the pattern $\mathcal{O}(\mathbf{c}_\perp)$ it suffices to investigate the projection images of the Voronoi domain $V(\mathbf{0})$ and its boundaries in $\mathbb{E}_\perp$.

One consequence of this analysis is immediate: all $\pi_\perp(P)$ for which the corresponding $\pi_\perp(\mathbf{q})+\pi_\perp(P^*)$ belong to the same vertex configuration [around $\pi_\perp(\mathbf{q})$] must have a common overlap in $\mathbb{E}_\perp$. The possible overlaps are convex polygons, called elementary polygons, which subdivide $\pi_\perp(V(\mathbf{0}))$. Furthermore, they represent the possible vertex configurations of the ideal quasiperiodic pattern one to one. An inspection of $\pi_\perp(V(\mathbf{0}))$ together with the projected boundaries in Fig. 2 yields, up to D_8 opera-

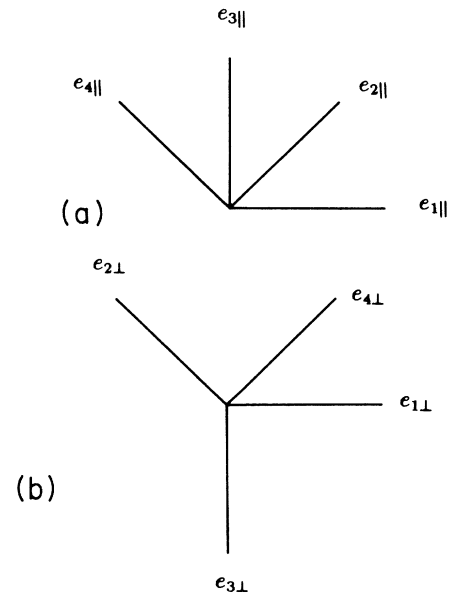

FIG. 1. Projection of the 4D basis into (a) $\mathbb{E}_\parallel$ and (b) $\mathbb{E}_\perp$.

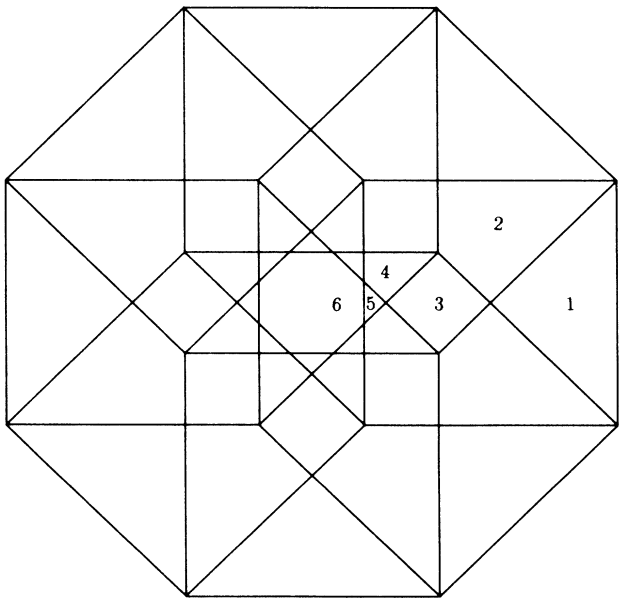

FIG. 2. Projection of the Voronoi domain of the $\mathbb{Z}^4$ lattice and its boundaries into $\mathbb{E}_\perp$. The numbering of the representative elementary polygons refers to the vertex configurations of Fig. 3.

tions, just six different elementary polygons each of which stands for one of the six possible vertex configurations in Fig. 3.

One can go even further. The space $\mathbb{E}_\parallel$ is not contained in a net plane of the lattice $\mathbb{Z}^4$. Hence, the projection images of the lattice points are dense and uniformly distributed in $\mathbb{E}_\perp$. Consequently,

$$\{\mathbf{c}_\perp - \pi_\perp(\mathbf{q}) | \mathbf{q} \in \mathbb{Z}^4\} \cap \pi_\perp(V(\mathbf{0}))$$

is dense and uniformly distributed in $\pi_\perp(V(\mathbf{0}))$, so precisely the fraction $A(\mathcal{E})/A(\pi_\perp(V(\mathbf{0}))$, where $A(x)$ is the area of x, of all vertices of the infinite pattern $\mathcal{O}(\mathbf{c}_\perp)$ are from the class represented by the elementary polygon $\mathcal{E} \subseteq \pi_\perp(V(\mathbf{0}))$. These areas are easy to determine analytically, the resulting relative frequencies of the vertex configuration classes are listed in Table II (we have added up all contributions from the corresponding D_8 orbits).

A very simple but effective algorithm for the construction of $\mathcal{O}(\mathbf{c}_\perp)$ can be extracted from the procedure explained above. This algorithm has been introduced in[3] and applied to patterns with fivefold symmetry. It is, in a natural way, adapted to the dualization scheme and works very economically. As this procedure is very general, we will demonstrate it for the octagonal pattern in some detail. The transcription to other examples will then be obvious.

Without loss of generality, we may assume one vertex to be positioned at $0 \in \mathbb{E}_\parallel$. Then, the following prescription provides arbitrarily large patches of the pattern $\mathcal{O}(\mathbf{c}_\perp)$ as in Fig. 4. (1) Choose $\mathbf{c}_\perp \in \pi_\perp(V(\mathbf{0}))$, so that indeed the initial vertex configuration surrounds $\mathbf{0}$ in $\mathbb{E}_\parallel$. (2) If $\pi_\perp(\mathbf{q})$ $(\mathbf{q} \in \Gamma)$ is a vertex of the pattern obtained so far whose configuration is not completely known, one finds the elementary polygon in $\pi_\perp(V(\mathbf{0}))$ that contains $\mathbf{c}_\perp - \pi_\perp(\mathbf{q})$. This determines the vertex configuration around $\pi_\perp(\mathbf{q})$ and yields new vertices of the pattern together with their preimages in Γ. (3) Proceed with step (2) with all incompletely known vertices until the tiling reaches the size desired.

TABLE II. The relative frequencies of the six allowed vertices. The numbering refers to Fig. 3, $\lambda = 1+\sqrt{2}$ is the silver number.

No. of vertex	Relative frequency	Approximate value
1	$-2+\lambda$	0.414
2	$10-4\lambda$	0.343
3	$-24+10\lambda$	0.142
4	$58-24\lambda$	0.059
5	$-70+29\lambda$	0.012
6	$29-12\lambda$	0.029

The set of forbidden $\mathbf{c}_\perp$ (see above) is of measure zero in $\pi_\perp(V(\mathbf{0}))$ and does not contain the points $\pi_\perp(\mathbb{Z}^4) \cap \pi_\perp(V(\mathbf{0}))$, the latter guaranteeing patterns with global D_8 symmetry. (In fact, Fig. 4 is obtained from $\mathbf{c}_\perp = 0$). It should be mentioned that every member of the local isomorphism class that $\mathcal{O}(\mathbf{0})$ belongs to possesses generalized D_8 symmetry, for details see Refs. 9 and 21.

Although we will not discuss the matching rules for the octagonal quasilattice (they can be found in Refs. 15 and 16) we would like to spend some time on a certain kind of symmetry of the pattern that has not yet been mentioned in this article: the deflation-inflation transformation. Let us consider the linear transformation

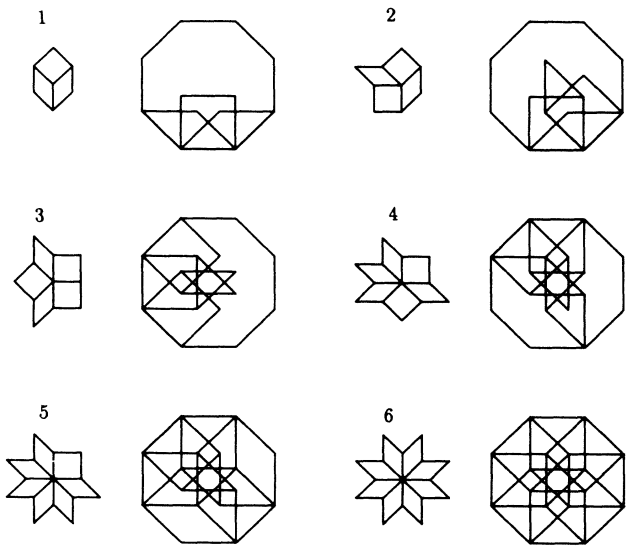

FIG. 3. The six vertex configurations of the ideal octagonal pattern as obtained from $\mathbb{Z}^4$ on the left and their dual polygons in the shadow of the Voronoi domain in $\mathbb{E}_\perp$ on the right. All polygons have a common overlap, the areas of which correspond to the relative frequencies of the vertex configurations in the ideal pattern.

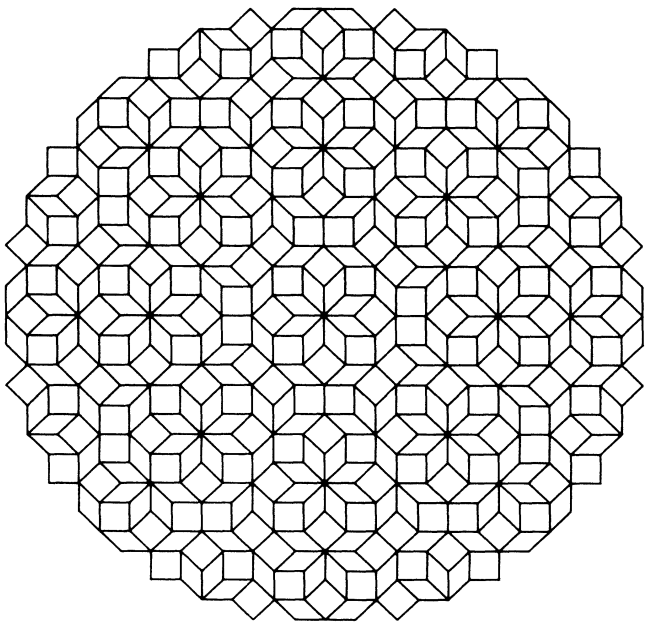

FIG. 4. Quasiperiodic octagonal pattern as obtained from the lattice $\mathbb{Z}^4$. The start parameter, with respect to the construction algorithm (cf. Sec. II) is $c_\perp = 0$.

$$\mathbf{e}_i \rightarrow \mathbf{e}_i' = \mathbf{e}_j M_{ji}, \quad M \equiv \begin{pmatrix} 1 & 1 & 0 & -1 \\ 1 & 1 & 1 & 0 \\ 0 & 1 & 1 & 1 \\ -1 & 0 & 1 & 1 \end{pmatrix}, \tag{2.10}$$

which leaves the lattice $\mathbb{Z}^4$ invariant because $M \in \mathrm{Gl}(4,\mathbb{Z})$, the group of unimodular 4×4 matrices.[18] A special property of M is

$$UMU^{-1} = \mathrm{diag}\left[\lambda, \lambda, -\frac{1}{\lambda}, -\frac{1}{\lambda}\right], \tag{2.11}$$

where $\lambda = 1+\sqrt{2}$ is the silver number, and, consequently,

$$[R(\mathbf{g}), M^k] = 0, \quad \mathbf{g} \in D_8, k \in \mathbb{Z}. \tag{2.12}$$

$\mathcal{C} = \{M^k | k \in \mathbb{Z}\} \cong \mathbb{Z}$ forms an infinite abelian subgroup of $\mathrm{Gl}(4,\mathbb{Z})$ the transformations of which have a certain meaning for the octagonal pattern because they act as rescaling transformation in $\mathbb{E}_\parallel$ and $\mathbb{E}_\perp$ separately. It turns out that

$$\mathcal{C} \cong \mathrm{cent}_{\mathrm{Gl}(4,\mathbb{Z})}(D_8)/\mathrm{cent}(D_8), \tag{2.13}$$

i.e., $\mathcal{C}$ is isomorphic with the factor group of the centralizer of D_8 in $\mathrm{Gl}(4,\mathbb{Z})$ divided by the center of D_8. Of course, even more general transformations could be important, namely the group

$$\mathcal{G} = \{M \in \mathrm{Gl}(4,\mathbb{Z}) | [\pi_\parallel, M] = 0\}. \tag{2.14}$$

Note that $[\pi_\parallel, M] = 0$ implies $[\pi_\perp, M] = 0$ since $\pi_\parallel + \pi_\perp = 1$. Obviously,

$$D_8 \otimes \mathcal{C} \subseteq \mathcal{G}, \tag{2.15}$$

and, moreover, $D_8 \otimes \mathcal{C}$ is a real subgroup of $\mathcal{G}$. The latter additionally contains elements like

$$\begin{aligned} &M = \mathrm{diag}(\lambda, 1/\lambda, -1/\lambda, -\lambda) \\ &\text{or } M = \mathrm{diag}(1, \lambda, 1, -1/\lambda) \end{aligned} \tag{2.16}$$

and powers, given in the reduced basis, cf. Eq. (2.5). There is even an interesting group in between, $\mathcal{N}$, which is

$$\mathcal{N} \cong \mathrm{norm}_{\mathcal{G}}(D_8)/D_8 \tag{2.17}$$

and one has

$$D_8 \otimes \mathcal{C} \subseteq D_8 \otimes_s \mathcal{N} \subseteq \mathcal{G}, \tag{2.18}$$

where $D_8 \otimes_s \mathcal{N}$ is the largest subgroup of $\mathrm{Gl}(4,\mathbb{Z})$ that is compatible with splitting into $\mathbb{E}_\parallel$ and $\mathbb{E}_\perp$ and with the generalized point symmetry[9] of the pattern obtained from the Klotz construction. The group $D_8 \otimes \mathcal{C}$ (or the group $D_8 \otimes_s \mathcal{N}$) might be considered as an extension of the ordinary point symmetry of the quasilattice (the 4D origin is left fixed), while $\mathcal{G}$ takes over the role of the unimodular group. In fact,

$$\mathcal{M} = \{\pi_\parallel(\mathbf{q}) | \mathbf{q} \in \mathbb{Z}^4\} \tag{2.19}$$

is a free module, generated by four elements over $\mathbb{Z}$. As much, $\mathcal{M}$ has an invariant group isomorphic with $\mathrm{Gl}(4,\mathbb{Z})$ itself, but not all of its elements are compatible with linear continuation in $\mathbb{E}_\parallel$. The subgroup of those which are is isomorphic with $\mathcal{G}$ and characterized by Eq. (2.14). In the case of an n-D lattice with the holohedry instead of D_8, $\mathcal{C}$ becomes trivial and $\mathcal{G}$ the unimodular group of that lattice that is isomorphic with $\mathrm{Gl}(n,\mathbb{Z})$.

The additional deflation-inflation "symmetry" has played an important role in the theory of quasicrystals because it is deeply connected to finding a consistent indexing for the diffraction spots that live on a module invariant with respect to the group $\mathcal{C}$. For the octagonal quasilattice discussed in this article, one has also local deflation-inflation rules,[15,21] which in general are not guaranteed by the existence of a linear transformation like M in Eq. (2.10). Let us now come back to the main path of the article, turning to the introduction of a certain class of defects.

III. THE ELASTIC ENERGY MEASURE FOR GEOMETRIC DEFECTS OF THE FIRST KIND

The description of ideal patterns that are free of defects is rather complete, the description of real patterns is still to be done: usually they are full of defects. An exhaustive treatment of this problem, especially with realistic decorations of the tiles, is far beyond the scope of this article (the interested reader is referred to Refs. 22 and 23, where topological classifications of defects by means of higher-dimensional crystallography are presented). But already the purely geometric structure gives rise to several defect models, one of which will be discussed in what follows. To this end, we introduce the notation "geometric defects." If we find in a pattern vertex configurations not contained in Fig. 4 we call them geometric defects. If they are still built from the tiles of the ideal pattern, we call them "geometric defects of the first kind," otherwise, if new tiles occur, "geometric defects of the second kind." Of course one might see similarities with the treatment of quasicrystals via the method of random tilings, where Ref. 24 is an example for a scenario with only geometric defects of the first kind, while Ref. 12 also includes the second kind. Nevertheless, our approach makes no reference at all to the liquid phase or a phenomenologic ansatz for the energy and, thus, seems to be more elementary. If what follows, we present an approach to the geometric defects of the first kind for the octagonal quasilattice and derive first thermodynamic consequences.

Let us start from the two tiles of our pattern, the square and the 45° rhomb, combinatorically: modulo orientation or reflection, one finds 16 possibilities to complete a vertex surrounding without gaps and overlaps. Six of them are those of Fig. 3, the ten missing ones are shown in Fig. 5. It is easy to see that all of them can be integrated into a patch of the octagonal quasilattice using local rearrangements without using tiles of a different shape. Hence, these ten objects are the candidates for the geometric defects of the first kind. Let us consider such a vertex configuration, i.e., any out of the list of the 16 possible ones, and let us assume this vertex to be part of an

octagonal pattern without gaps or overlaps. Then, each tile of our vertex configuration has a uniquely defined preimage, i.e., a 2D boundary of the dual complex. All of them share a common 4D lattice point, the preimage of our vertex point. Consequently, the set of dual 2D boundaries, which are 2D boundaries of the Voronoi complex, must lie within the same Voronoi cell, namely that one dual of the 4D lattice point just mentioned. Therefore, one can geometrize the scenario of the geometric defects of the first kind within the ordinary Voronoi cell that is a nontrivial result and would not be at all valid for the geometric defects of the second kind. The next step is the transition from the geometric picture to energetic considerations.

By means of the dualization scheme, we will now introduce an elastic measure which, locally, gives the amount of energy one has to pay for the "forbidden" vertices. From the geometry, we know that the whole analysis can be carried out within $\pi_\perp(V(\mathbf{0}))$. Every vertex configuration of Fig. 5 can be seen as the projection of appropriate 2D boundaries P_i^*, $1 \le i \le r$, where r is the number of tiles surrounding the vertex point. Now, we consider the set $\{\pi_\perp(P_i) | 1 \le i \le r\}$ of tiles in the perpendicular space. Without loss of generality, we may assume the whole set to belong to the 2D boundaries of $V(\mathbf{0})$, and this is shown in Fig. 5 as well. Obviously, not all the $\pi_\perp(P_i)$ can have a common overlap because this would give us back the vertices of Fig. 3.

Now, the question is what can this geometric scenario tell us about the degree of deviation from the ideal pattern. A combination of pairwise overlaps of the $\pi_\perp(P_i)$'s, as proposed in Ref. 25 for the icosahedral phase, does not result in a differentiation between ideal vertices and defects. Hence, we go back to a function, first proposed by Kramer,[26] which measures a specific type of minimal square distance in perpendicular space:

$$\Delta E = \min_{x_{\perp,i} \in \pi_\perp(P_i)} \left[\frac{E_0}{a^2} \sum_{i<j} (x_{\perp,i} - x_{\perp,j})^2 \right], \tag{3.1}$$

where a is the lattice constant and E_0 a free-energy parameter. ΔE vanishes for the allowed vertices: one can take all $x_{\perp,i}$ from the common overlap. $\Delta E > 0$ for all other vertices, as can be seen from Fig. 5. ΔE can be calculated analytically, the results are listed in Table III. A typical example of a minimizing point configuration $x_{\perp,i}$ is given in Fig. 6.

It turns out that ΔE is degenerate only for the ideal vertices, the defects are brought into a unique sequence. Partially, this sequence seems to be plausible since strongly crystallographic configurations like No. 7 cost a lot, but this simple picture is too naive and has to be replaced by a more reliable calculation that simultaneously justifies the choice of ΔE as energy measure. This will be achieved by some simple first-step stability calculations based on a truncated Lennard-Jones potential as used in Ref. 27:

$$V_{\mathrm{LJ}}(\mathbf{r}) = \begin{cases} E\left[\left(\frac{\sigma}{r}\right)^{12} - \left(\frac{\sigma}{r}\right)^{6}\right] \cos^2\left[\frac{\pi}{2}\frac{1}{\beta}\frac{r}{\sigma}\right], & \text{if } 0 < \frac{r}{\sigma} < \beta \\ 0, & \text{if } \frac{r}{\sigma} \ge \beta , \end{cases} \tag{3.2}$$

where r denotes the distance $|r_i - r_j|$ between the atoms i and j and β a truncation factor (here, $\beta = 2$). The minimum of the potential can be positioned by means of σ. E is an arbitrary energy scale factor. For a diatomic system, β, σ, and E have to be replaced by β_{ab}, σ_{ab}, E_{ab} etc., for more details see Ref. 27. To compare this Lennard-Jones system with the elastic measure ΔE introduced above we proceed as follows.

The first step is to choose a decoration of the planar octagonal picture. A simple decoration of the vertices with one sort of atoms leads to unsatisfactory results, i.e., the defective patterns sometimes are energetically more favored than the ideal ones. But this is no surprise since every 2D pattern with a monoatomic decoration and an isotropic, scalar potential like V_{LJ} will relax to the ordinary honeycomb lattice.[28] On the other hand, the forbidden eightfold symmetry was discovered in the binary alloy NiCr.[14] So it is more reasonable to take a two-atom decoration. To this end, one sort of atom is placed at the center of the squares, the other one at the center of the rhombi. For this decoration, the free parameters σ_{aa}, σ_{bb} are optimized on the ideal pattern by means of Monte Carlo calculations. Only two of the three possible σ_{ij} are linearly independent because of

$$\sigma_{aa} = r_a + r_a, \quad \sigma_{ab} = r_a + r_b, \quad \sigma_{bb} = r_b + r_b , \tag{3.3}$$

where r_i are the radii of the "single potential" belonging to the two different atoms. The possible energy scale factors E_{ij} and the truncation factors β_{ij} are chosen to be equal, respectively. With the optimized parameters, the potential energy of the decorated ideal and the defect patterns are calculated. The difference ΔV_{LJ} of both is to be compared with ΔE for the different defects. Unfortunately, it is not possible to place a geometric defect of the first kind into the pattern separately without incorporating additional ones in the neighborhood (except No. 15). Therefore, only defect clusters can be compared.

As there are two energy scale factors E, E_0 in both calculations only the relative values $\Delta V_{\mathrm{LJ}}/E$ and $\Delta E/E_0$

are shown in Table IV. Despite remarkable similarities in both cases the order of precedence in Table IV is not equal. This is due to the fact that the elastic measure takes only one vertex into account, whereas the Lennard-Jones potential is sensitive to the next-to-nearest-neighbor vertices. In a sense the elastic energy measure ΔE can be seen as a mean-field approximation of the contribution of the forbidden vertex configurations to the total energy.

Nevertheless, this simple approach justifies the definition of the energy measure ΔE. The discrepancy between both measures can be interpreted in two different ways. On the one hand, it can be seen as a lack of the elastic measure ΔE introduced above. It is obvious that ΔE can only be seen as an average contribution for the single defects that nevertheless should well described the qualitative behavior away from any phase transitions. On the other hand, it is possible to question the reliability of isotropic, scalar potentials like V_{LJ} for two-component systems like alloys, but it is far beyond the scope of this section to derive more subtle and more realistic models that had to incorporate molecular-dynamics calculations.

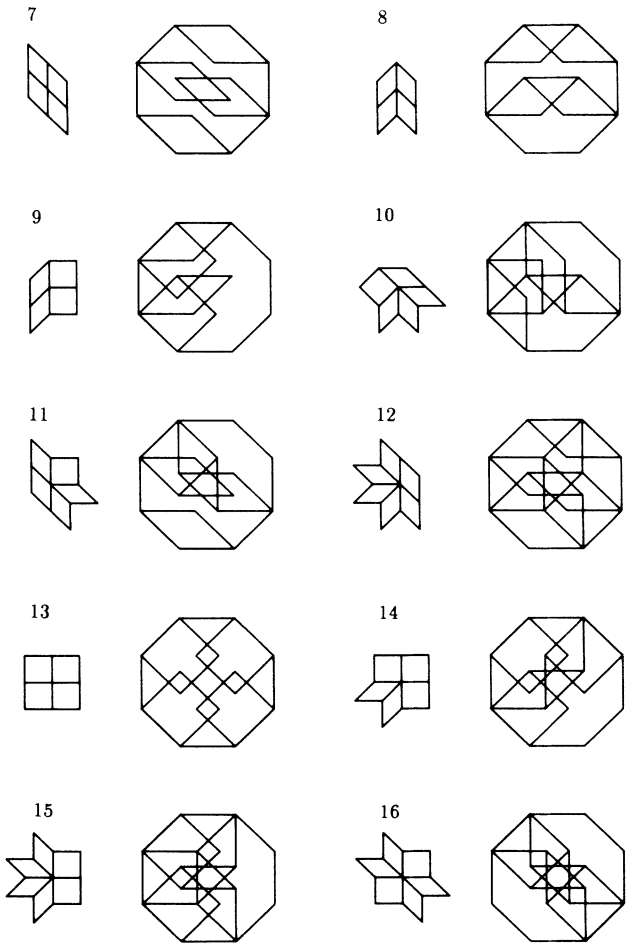

FIG. 5. The ten forbidden vertices (geometric defects of the first kind) of the octagonal pattern (left) and their dual polygons in the shadow of the Voronoi domain in $\mathbb{E}_\perp$ (right), respectively.

TABLE III. The energy measure ΔE of the ten forbidden vertices. The numbering refers to that of Fig. 5. The 4D lattice constant is $a=1$.

No. of vertex	$\Delta E/E_0$	Approximate value
7	$6-2\lambda$	1.17
8	$\frac{1}{3}$	0.33
9	$\frac{2}{3}(5-2\lambda)$	0.11
10	$\frac{5}{6}(5-2\lambda)$	0.14
11	$\frac{1}{8}(27-10\lambda)$	0.36
12	$\frac{1}{7}(132-54\lambda)$	0.23
13	$2(5-2\lambda)$	0.34
14	$\frac{5}{4}(5-2\lambda)$	0.21
15	$\frac{1}{2}(29-12\lambda)$	0.01
16	$\frac{3}{2}(5-2\lambda)$	0.26

IV. THERMODYNAMIC CONSEQUENCES OF ΔE FOR THE SPECIFIC HEAT

Because of the higher-dimensional background, it is plausible that quasicrystals should have additional degrees of freedom in comparison with ordinary crystals. This is usually described by means of phasons in the Landau theory of phase transitions from the liquid-to-solid phase.[10,11] However, as mentioned in the Introduction, we would like to avoid this phenomenologic description and start from the classification of the geometric defects of the first kind together with the energy measure ΔE instead. This way, we do not make reference to the liquid phase, except the idea that performed clusters might be an explanation for the preference of the ideal tiles. Note

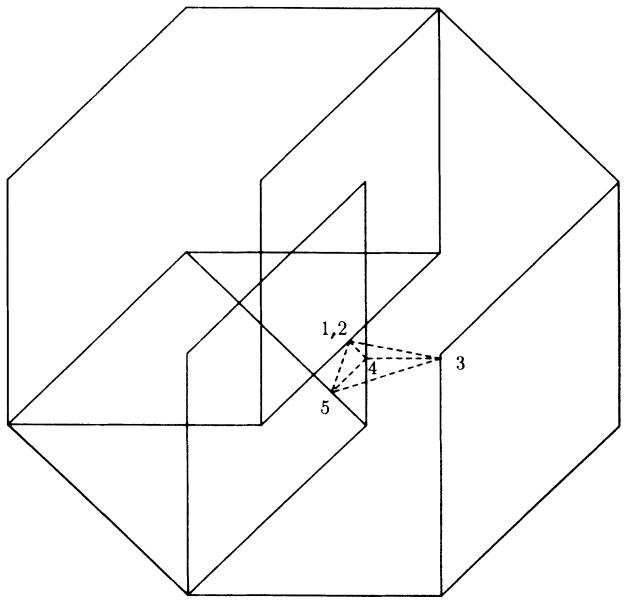

FIG. 6. The dual polygons of vertex No. 11 in the shadow of the Voronoi domain in $\mathbb{E}_\perp$ and the minimal point configuration of the elastic energy measure ΔE connected by lines.

TABLE IV. The difference ΔV_{LJ} of the potential energy between the ideal and defective vertex configurations using a truncated Lennard-Jones potential in comparison to the results of the energy measure ΔE. The 4D lattice constant is $a=1$. The vertex configurations (numbered from 1 to 13) are different patches that do not occur in the ideal octagonal pattern. They consist of allowed (Fig. 3) and (up to 14) forbidden vertices (Fig. 5) and are placed into the ideal pattern. All defects of Fig. 5 are incorporated. The configurations Nos. 1 and 2 only consist of allowed vertices, whereas No. 3 consists of only one defect of the first kind (No. 15 of Fig. 5).

Vertex configuration	$\Delta E/E_0$	$\Delta V_{LJ}/E$
1	0	0.00
2	0	0.07
3	0.01	0.56
4	0.51	1.10
5	0.74	1.99
6	0.78	2.24
7	1.27	2.79
8	1.28	3.38
9	1.41	3.86
10	1.56	2.86
11	2.31	4.36
12	2.53	4.33
13	3.58	5.42

that an ordinary crystal that is built from a single fundamental cell cannot show geometric defects of the first kind. Hence, these defects reflect the additional degrees of freedom possible in quasicrystals. Nevertheless, these structures can be seen in a unified way by means of higher-dimensional crystallography and defects,[23] but that does not help for our purposes.

Let us now introduce the Boltzmann factor for a vertex configuration v of N vertices, $e^{-[\Delta E(C)/kT]}$, where $\Delta E(C)$ is the energy measure of Eq. (3.1). Regarding the vertex configuration within a canonical ensemble, the partition function can be written down:

$$Z_N=\sum_C e^{-\beta\Delta E(C)}\,, \tag{4.1}$$

$$\Delta E(C)=\sum_{v\in C}\Delta E_v;\ \beta=1/kT\,, \tag{4.2}$$

i.e., for a given N, as a sum over all possible arrangements of N vertices. Of course, only those arrangements are taken into account, the vertices of which are pairwise connected by bonds.

Following the canonical way[29] we can now calculate the thermodynamic variables like the free energy f, internal energy u, and the specific heat c_V for our defect system,

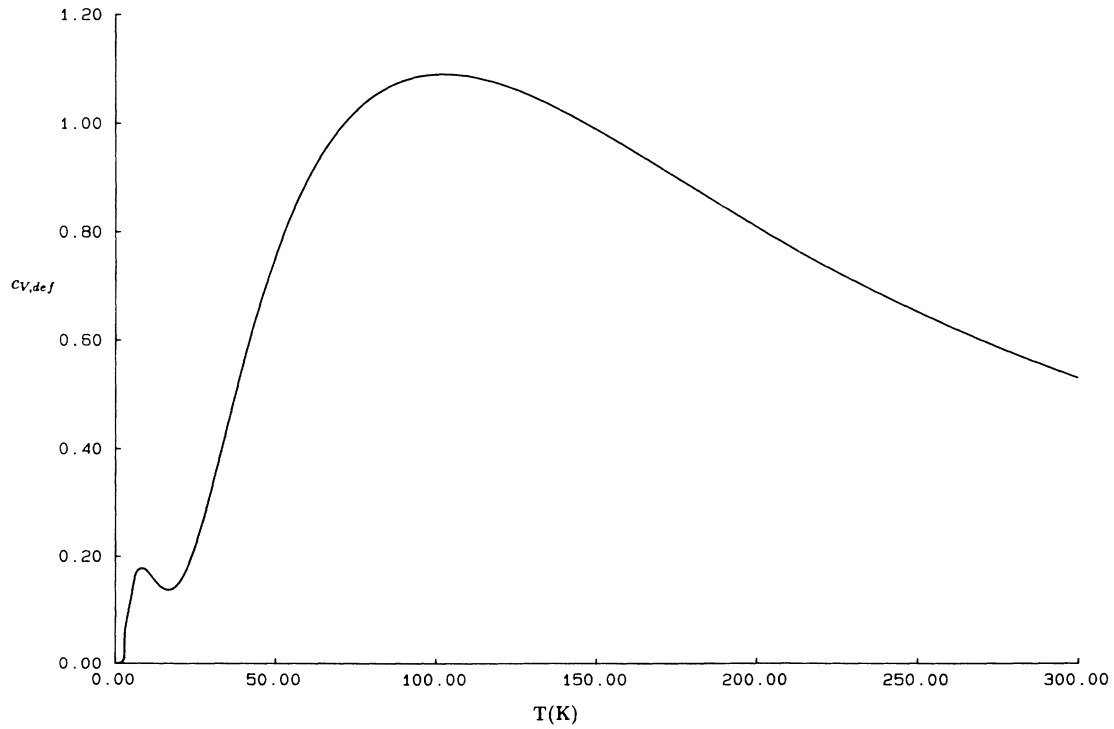

FIG. 7. The defect contribution $c_{V,\mathrm{def}}$ of the specific heat corresponding to Eq. (4.5) obtained from the $N=2$ canonical vertex ensemble ($E_0=0.1$ eV, $a=4$D lattice constant).

$$f_{\text{def}} = -\beta^{-1}\ln(Z_N) , \tag{4.3}$$

$$u_{\text{def}} = -\frac{\partial}{\partial\beta}\ln(Z_N) , \tag{4.4}$$

$$c_{V,\text{def}} = k\beta^2\frac{\partial^2}{\partial\beta^2}\ln(Z_N) . \tag{4.5}$$

For a given N, the number of all possible vertex configurations that contribute to Z_N is very large. To get a first impression of the behavior of the thermodynamic variables we calculate the $N=2$ configurations as a rough approximation of the 2D octagonal quasicrystal. Even in this case there are more than 200 different combinations of the 16 vertices possible. Of course, $N=2$ is only a crude approximation of a real quasicrystal, wherefore the results will only have a qualitative meaning. But experience with other nearest-neighbor models (like the Ising model) and the finite-size investigation of the Fibonacci quasicrystal (cf. Appendix) show that even at $N=2$ a qualitative understanding of the behavior of the physical system can be achieved.

Figure 7 shows the result for the defect contribution to the specific heat c_V per site. The parameter E_0 in the energy measure, which corresponds to a local excitation energy in the perpendicular space, was chosen to be $E_0=0.1$ eV, the parameter a is the 4D lattice constant. The first small maximum of c_V is due to the existence of vertex No. 15, which is by far the cheapest to be builtin (cf. Table III) and has, therefore, a large contribution to the specific heat at low temperatures. It is most probably a finite-size effect. Unfortunately, it was not possible to make calculations of the behavior of c_V in the thermodynamic limit $N\to\infty$ (cf. Appendix).

The ansatz for the energy measure contains only one free parameter, E_0, which determines the strength of the defect specific heat (assuming a is fixed by the lattice constant). In order to see whether this contribution is a detectable effect or not one has to compare it with the ordinary phonon term as realized in a simple manner by the Einstein ansatz[29]

$$c_{V,\text{phon}} = \frac{x^2e^x}{(e^x-1)^2};\ x=\frac{\Theta_E}{T} . \tag{4.6}$$

Here, we suppose that the phonon contribution is well approximated by the formulas well known from the crystalline phase. Figure 8 shows $c_{V,\text{phon}}$ for $\Theta_E=180$ K, $c_{V,\text{def}}$ (as above) and the sum, $c_V=c_{V,\text{phon}}+c_{V,\text{def}}$, assuming approximately the independence of the phonon and the defect term. Taking the parameters as quoted above, the defect term of c_V results in a significant rise with respect to the phonon term alone that should be detectable. As mentioned at the beginning of this section, this might be a consequence of the higher number of degrees of freedom possible in quasicrystals that are well established in other branches, e.g., neutron scattering.[30]

V. CONCLUSION

For the 2D primitive octagonal quasilattice, we have presented a rigorous geometric approach to the combinatorically possible vertex configurations. Within the duali-

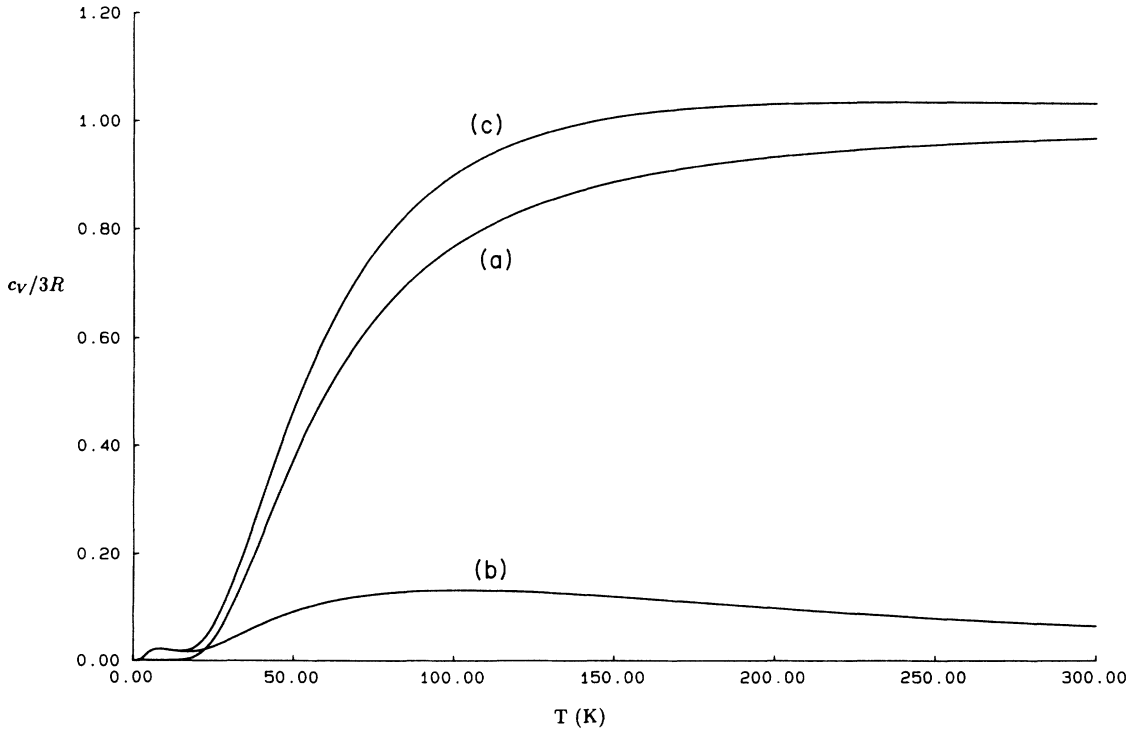

FIG. 8. (a) The phonon term of the specific heat corresponding to the Einstein ansatz in Eq. (4.6) ($\Theta_E=180$ K). (b) (The defect term of Fig. 7. (c) The sum of (a) and (b).

zation scheme, they are treated as geometric defects of the first kind and represent a (finite) number of degrees of freedom a quasicrystal should have in contrast to its periodic, crystalline relative. If so, this should be detectable in simple thermodynamic quantities like the specific heat, c_V. As a simple model, we have calculated an elastic energy measure in perpendicular space that can be seen as a mean-field contribution of the single defects to the total energy of the (complete) configuration. Assuming the quasicrystal to be in its thermodynamic equilibrium we have calculated c_V from the canonical partition function Z_N with $N=2$. As shown by the Fibonacci chain as a toy model, this may serve as a qualitative picture, but most probably not as a quantitative one. Nevertheless, for some plausible "perpendicular" excitation energy E_0, one finds an additional contribution to the specific heat that should qualitatively explain c_V to be significantly higher than in the crystalline case. This phenomenon seems to be seen in experiment.[31]

However, a more detailed calculation along the lines presented above has to be done, especially for other quasicrystals (like the icosahedral one, where one has to face the large number of possible configurations[5]) and with better approximations of the thermodynamic limit.

ACKNOWLEDGMENTS

This article grew out of a cooperation between the authors, P. Kramer, M. Schlottmann, Tübingen, S. I. Ben-Abraham, Beer-Sheba, and P. D. Jarvis, Hobart. Furthermore, we have benefitted from discussions with Ph. Butler, P. Delbourgo, and J.-B. Suck. Financial support from Deutsche Forschungsgemeinschaft, Australian Research Council and Alfried Krupp von Bohlen und Halbach-Stiftung is gratefully acknowledged.

APPENDIX: THE FIBONACCI CHAIN AS TOY MODEL

As is well known,[8,9] the Fibonacci chain can be obtained from the 2D square lattice by means of a cut through the corresponding Klotz complex along the line with slope $\tan\alpha=1/\tau$, $\tau=(1+\sqrt{5})/2$. One gets a quasiperiodic tiling with intervals of the length $\sin\alpha$ (short, S) and $\cos\alpha$ (long, L), respectively. The possible vertices are LL (with the frequency $\nu=1/\tau^2\cong 38.2\%$) and LS and SL (together with $\nu=1/\tau\simeq 61.8\%$), which can be obtained by the same methods described above. The vertex SS does not occur in the ideal Fibonacci chain and thus turns out to be the only geometric defect of the first kind. The energy measure analogous to Eq. (3.1) can easily be calculated,

$$\Delta E(v)=\begin{cases}0, & \text{if } v\in(\mathrm{LL},\mathrm{LS},\mathrm{SL})\\ E_0\tfrac{1}{5}(7-4\tau), & \text{if } v\in(\mathrm{SS})\end{cases}, \tag{A1}$$

where we have taken the lattice constant $a=1$. We will use the abbreviation $d=(7-4\tau)/5$ from now on.

Let us consider the ensemble of cyclically closed, finite chains with precisely N vertices. We define the partition function

$$Z_N=\sum_C e^{-\beta\Delta E_{\mathrm{tot}}(C)}, \tag{A2}$$

with $\beta=1/kT$ and $\Delta E_{\mathrm{tot}}(C)=\sum_{v\in C}\Delta E(v)$. For a given

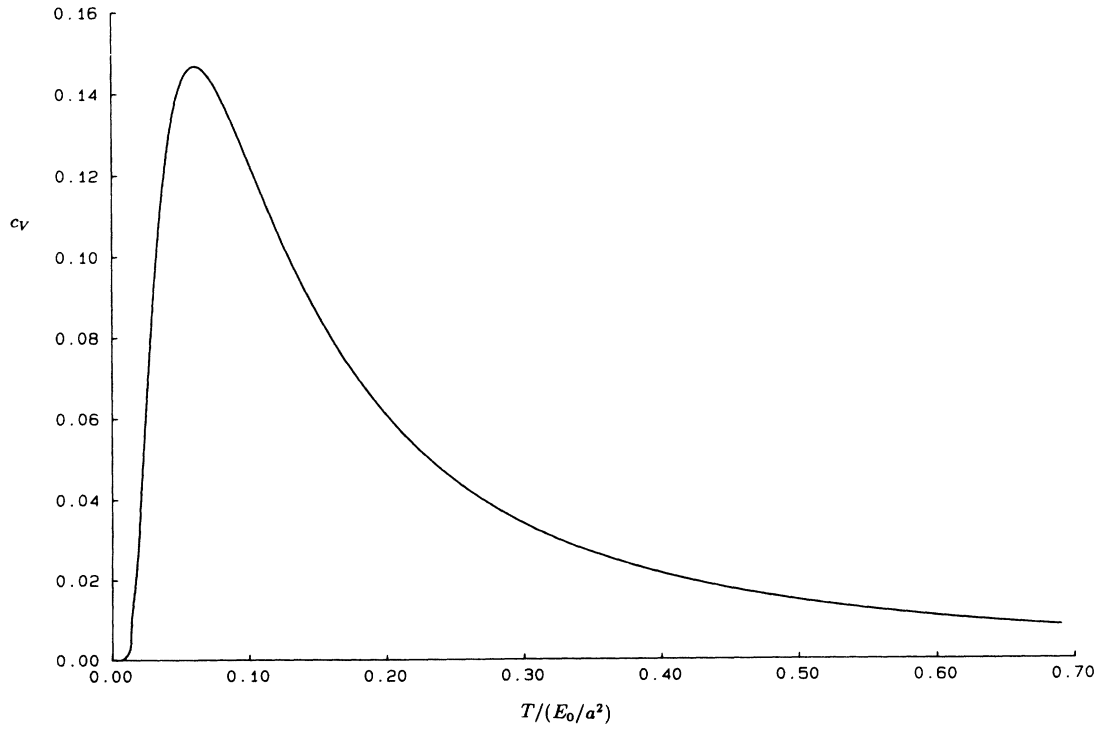

FIG. 9. The defect term $c_{V,\mathrm{def}}$ [Eq. (A12)] of the specific heat for the Fibonacci quasilattice in arbitrary units.

configuration C, the expression $\Delta E_{\text{tot}}(C)$ is to be seen as its total energy. The structure suggests a mapping to the exactly solvable Ising model:[32]

$$E(\sigma)=-J\sum_{j=1}^{N}\sigma_j\sigma_{j+1}-\frac{H}{2}\sum_{j=1}^{N}(\sigma_j+\sigma_{j+1}) , \quad \text{(A3)}$$

$$\sigma_{N+1}=\sigma_1, \quad \sigma_j\in\{+1,-1\} . \quad \text{(A4)}$$

Here, every interval between two vertices hosts a spin variable with value $+1$ for S and -1 for L, and the number of intervals equals the number of vertices due to periodic boundary conditions. The idea is now to exactly replace the contribution $\Delta E(\mathbf{v})$ of a vertex $\mathbf{v}$ by the interaction energy of neighboring spins. The vertices LL, LS, and SL must be represented by the same value that results in the condition $H/2J=+1$. We may add a constant contribution to Eq. (A3) and find the partition function

$$Z_N=\sum_{\sigma}\exp\left[K\sum_{j}\left[\sigma_j\sigma_{j+1}+\frac{h}{2}(\sigma_j+\sigma_{j+1})\right]\right]e^{NK} , \quad \text{(A5)}$$

which coincides with Eq. (A2) if

$$\frac{h}{2}=K=-\beta E_0 d/4 . \quad \text{(A6)}$$

Note that this approach is different from a model for magnetic behavior (like Ref. 33) because the technique of spin variables is only used to calculate some geometric contributions. With the technique of transfer matrices, one obtains

$$Z_N=e^{KN}\mathrm{tr}V^N=e^N(\lambda_1^N+\lambda_2^N) , \quad \text{(A7)}$$

where

$$V=\begin{bmatrix} e^{K+h} & e^{-K} \\ e^{-K} & e^{K-h} \end{bmatrix} \quad \text{(A8)}$$

and

$$\lambda_{1,2}=e^K\cosh(K)\pm[e^{2K}\sinh^2(h)+e^{-2K}]^{1/2} . \quad \text{(A9)}$$

Since $\lambda_1\geq\lambda_2$ with equality only if $h=0$ and $K\to\infty$, we may use $(\lambda_2/\lambda_1)^N\to 0$ for $N\to\infty$ and simplify the expression for the thermodynamic limit

$$f=-\frac{1}{\beta}(\ln\lambda_1+K) , \quad \text{(A10)}$$

$$U=-\frac{1}{\lambda_1}\frac{\partial\lambda_1}{\partial\beta}-\frac{\partial K}{\partial\beta} , \quad \text{(A11)}$$

$$c_V=k\beta^2\left[\frac{1}{\lambda_1}\frac{\partial^2\lambda_1}{\partial\beta^2}-\frac{1}{\lambda_1^2}\frac{\partial\lambda_1}{\partial\beta}+\frac{\partial^2 K}{\partial\beta^2}\right] , \quad \text{(A12)}$$

for f, U, c_V the free energy, interval energy and specific heat per site, respectively. Figure 9 shows the specific heat that resembles that of the octagonal quasilattice. Of course, Eq. (A5) is exact also finite size, which allows the investigation of finite-size influences. For various parameters (E,T), our calculations showed that for any realistic parameter choice the thermodynamic limit was reached at $N=5$ within deviations of less than 10%. Even at $N=2$, the deviation did not exceed 20%. Looking back to the octagonal lattice, this finite size behavior indicates that the $N=2$ approximation of Sec. IV can be seen as qualitatively reliable because the correlation length is sufficiently small.

[1] *The Physics of Quasicrystals*, edited by P. J. Steinhardt and S. Ostlund (World Scientific, Singapore, 1987).

[2] *Aperiodicity and Order*, edited by M. V. Jarić (Academic, London, 1989), Vol. 2.

[3] M. Baake, P. Kramer, M. Schlottmann, and D. Zeidler, Int. J. Mod. Phys. B (to be published).

[4] C. L. Henley, Phys. Rev. B **34**, 797 (1986).

[5] S. I. Ben-Abraham (unpublished).

[6] M. V. Jarić, Phys. Rev. B **34**, 4685 (1986).

[7] P. Kramer and D. Zeidler, Acta Crystallogr. Sec. A **45**, 524 (1989).

[8] P. Kramer and M. Schlottmann, J. Phys. A **22**, L1097 (1989).

[9] M. Schlottmann (unpublished).

[10] P. Bak, Phys. Rev. D **32**, 5764 (1985).

[11] J.-C. Toledano and P. Toledano, *The Landau Theory of Phase Transitions* (World Scientific, Singapore, 1989).

[12] M. Widom, K. J. Strandburg, and R. H. Swendsen, Phys. Rev. Lett. **58**, 706 (1987).

[13] F. P. M. Beenker (unpublished).

[14] Z. M. Wang and K. H. Kuo, Acta Crystallogr. Sec. A **44**, 857 (1988).

[15] J. E. S. Socolar, Phys. Rev. B **39**, 10 519 (1989).

[16] B. Grünbaum and G. C. Shepard, *Tilings and Patterns* (Freeman, New York, 1987).

[17] M. Baake, D. Joseph, and M. Schlottmann (unpublished).

[18] H. S. M. Coxeter and W. O. J. Moser, *Generations and Relations for Discrete Groups*, 4th ed. (Springer, New York, 1980).

[19] M. Baake, B. Gemünden, and R. Oedingen, J. Math. Phys. **23**, 944 (1982); **24**, 1021 (1983); **25**, 3171 (1984).

[20] J. P. Serre, *Linear Representations of Finite Groups*, 2nd ed. (Springer, New York, 1982).

[21] K. Niizeki, J. Phys. A **22**, 1859 (1989).

[22] D. Levine *et al.*, Phys. Rev. Lett. **54**, 1520 (1985). J. Bohsung and H.-R. Trebin, Phys. Rev. Lett. **58**, 2277 (1987). J. Bohsung and H.-R. Trebin, in *Aperiodicity and Order*, edited by M. V. Jarić (Academic, London, 1989), Vol. 2.

[23] M. Kléman, J. Phys. (Paris) (to be published).

[24] C. L. Henley, in *Quasicrystals and Incommensurate Structures in Condensed Matter*, edited by M. J. Yacaman, D. Romen, and A. Gomez (World Scientific, Singapore, 1990).

[25] S. I. Ben-Abraham, in *Proceedings of The Adriatico Research Conference on Quasicrystals*, edited by M. V. Jarić and S. Lundquist (World Scientific, Singapore, 1990).

[26] P. Kramer (private communication).

[27] J. Roth, R. Schilling, and H.-R. Trebin, Phys. Rev. B **41**, 2735 (1990).

[28]J. Roth (private communication).
[29]R. K. Pathria, *Statistical Mechanics* (Pergamon, Oxford, 1988).
[30]J.-B. Suck (unpublished); J.-B. Suck (unpublished).
[31]J. Wosnitza, R. van den Berg, and H. V. Löhneysen, Z. Phys. **70**, 31 (1988); J.-B. Suck (private communication).
[32]R. J. Baxter, *Exactly Solved Models in Statistical Mechanics* (Academic, London, 1982).
[33]F. Vallet, R. Schilling, and S. Aubry, J. Phys. C **21**, 67 (1988).